

## REVIEW

[View Article Online](#)  
[View Journal](#) | [View Issue](#)Cite this: *Chem. Sci.*, 2024, 15, 8280Copper-catalyzed asymmetric allylic substitution of racemic/*meso* substratesJun Li,<sup>†a</sup> Junrong Huang,<sup>†ab</sup> Yan Wang,<sup>a</sup> Yuexin Liu,<sup>a</sup> Yuxiang Zhu,<sup>†\*c</sup> Hengzhi You<sup>†\*ab</sup> and Fen-Er Chen<sup>†\*abd</sup>

The synthesis of enantiomerically pure compounds is a pivotal subject in the field of chemistry, with enantioselective catalysis currently standing as the primary approach for delivering specific enantiomers. Among these strategies, Cu-catalyzed asymmetric allylic substitution (AAS) is significant and irreplaceable, especially when it comes to the use of non-stabilized nucleophiles ( $pK_a > 25$ ). Although Cu-catalyzed AAS of prochiral substrates has also been widely developed, methodologies involving racemic/*meso* substrates are highly desirable, as the substrates undergo dynamic processes to give single enantiomer products. Inspired by the pioneering work of the Alexakis, Feringa and Gennari groups, Cu-catalyzed AAS has been continuously employed in deracemization and desymmetrization processes for the synthesis of enantiomerically enriched products. In this review, we mainly focus on the developments of Cu-catalyzed AAS with racemic/*meso* substrates over the past two decades, providing an explicit outline of the ligands employed, the scope of nucleophiles, the underlying dynamic processes and their practical applications.

Received 1st April 2024

Accepted 6th May 2024

DOI: 10.1039/d4sc02135e

[rsc.li/chemical-science](https://rsc.li/chemical-science)

## 1. Introduction

There is a growing interest in the catalytic and enantioselective synthesis of intricate organic compounds using readily accessible materials.<sup>1–6</sup> Among them, AAS has emerged as a reliable approach for the synthesis of enantiomerically pure compounds. Since the pioneering work by the Trost group<sup>7–9</sup> on Pd-catalyzed AAS, transition metal-catalyzed AAS has been continuously developed as a powerful tool for the efficient construction of chiral C–C and C–X bonds.<sup>10–16</sup> Additionally, AAS has successfully enabled the total synthesis of various natural products and drugs.<sup>17–20</sup> This significant transformation was primarily driven by the utilization of second- and third-row transition metals, particularly Pd,<sup>21</sup> Rh,<sup>22</sup> and Ir,<sup>23</sup> which have become dominant catalysts in the total synthesis of numerous natural products. First-row transition metals are used less frequently in AAS reactions despite being more cost-effective and abundant alternatives to second- and third-row metals. Moreover, first-row metals often offer distinct reactivities and mechanistic possibilities compared to their second- and third-

row counterparts. Recently, copper has emerged as one of the predominant metal catalysts in metal-catalyzed AAS.<sup>24–32</sup> This review aims to elucidate the nomenclature associated with dynamic processes in Cu-catalyzed AAS and provide an overview of their recent advancements and applications in synthesizing enantioenriched molecules. In the first section, fundamental aspects of Cu-catalyzed AAS chemistry, ranging from general mechanisms to dynamic processes, will be discussed.

## 1.1 Cu-catalyzed asymmetric allylic substitution

Compared with Pd/Rh/Ir catalysis, Cu catalysis has its unique features.<sup>33,34</sup> Typically, non-stabilized organometallic nucleophiles ( $pK_a > 25$ ) including organozinc, organomagnesium, organolithium, organoaluminum or mild organoboron reagents, are commonly employed in Cu-catalyzed AAS. Recent extensive investigations have proposed a comprehensive mechanism for Cu-catalyzed AAS using hard nucleophiles (Scheme 1a). The first step involves transmetalation between the ligated copper(i) salt **A** and the organometallic species, resulting in the formation of the organocuprate species **B**. Upon coordination of **A** to the allyl substrate, this leads to the subsequent formation of  $\pi$ -complex **C**. Oxidative addition at the  $\gamma$ -position to the leaving group occurs on copper, yielding  $[\sigma + \pi]$ -allyl copper(III) species **D**. The newly formed  $[\sigma + \pi]$ -allyl complex **D** can undergo two competitive pathways depending on the nature of X, a non-transferrable substituent at the copper center in **D**: if X is an electron-withdrawing group such as CN or Cl, reductive elimination becomes favored and forms a branched product along with the regeneration of copper(i) salt

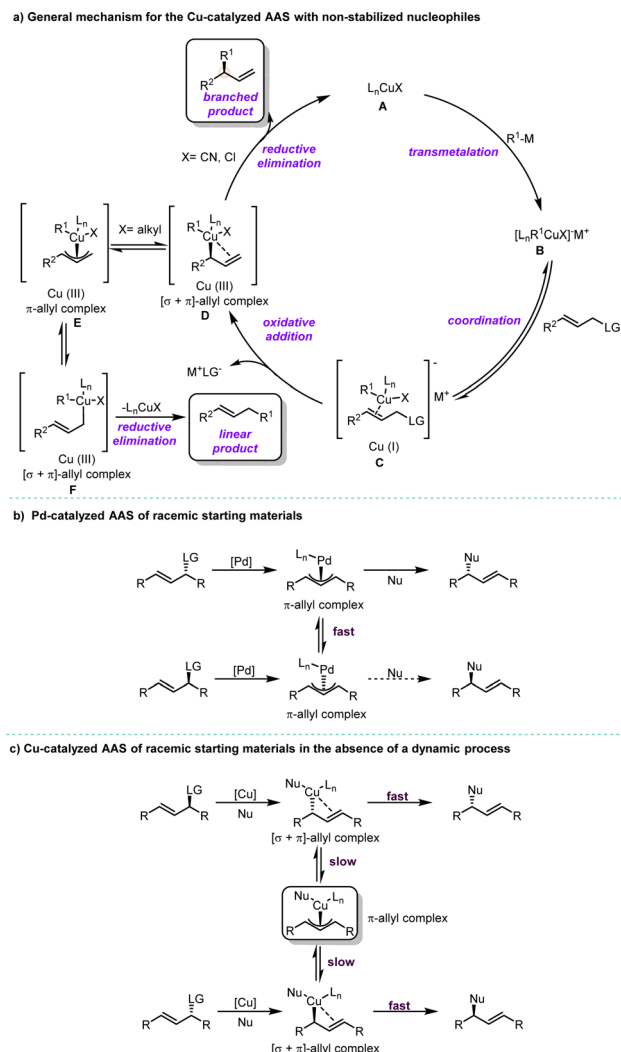
<sup>a</sup>School of Science, Harbin Institute of Technology (Shenzhen), Taoyuan Street, Nanshan District, Shenzhen, 518055, China. E-mail: youhengzhi@hit.edu.cn

<sup>b</sup>Green Pharmaceutical Engineering Research Center, Harbin Institute of Technology (Shenzhen), Taoyuan Street, Nanshan District, Shenzhen, 518055, China

<sup>c</sup>School of Pharmaceutical Sciences (Shenzhen), Shenzhen Campus of Sun Yat-sen University, Shenzhen, 518107, China. E-mail: zhuys86@mail.sysu.edu.cn

<sup>d</sup>Engineering Center of Catalysis and Synthesis for Chiral Molecules, Department of Chemistry, Fudan University, Shanghai, 200433, China. E-mail: rfchen@fudan.edu.cn

<sup>†</sup> These authors contributed equally: Jun Li and Junrong Huang.



**Scheme 1** (a) General mechanism for the Cu-catalyzed AAS with non-stabilized nucleophiles; (b) Pd-catalyzed AAS of racemic starting materials; (c) Cu-catalyzed AAS of racemic starting materials in the absence of a dynamic process.

A; however, if X is an electron-donating group like an alkyl substituent, isomerization from  $[\sigma + \pi]$ -allyl complex **D** via  $\pi$ -allyl complex **E** to  $[\sigma + \pi]$ -allyl complex **F** becomes feasible and results in a linear product. It should be noted that the regiochemical outcomes of reactions are dictated not only by the substituent X but also by factors such as steric effects and the presence of chelating groups on ligands, which control site selectivity during bond formation.<sup>35–40</sup> Additionally, it is crucial to precisely tune parameters including the structural and electronic properties of the electrophile, leaving group, and nucleophile, as well as reaction conditions such as solvent choice and temperature.<sup>11,33</sup>

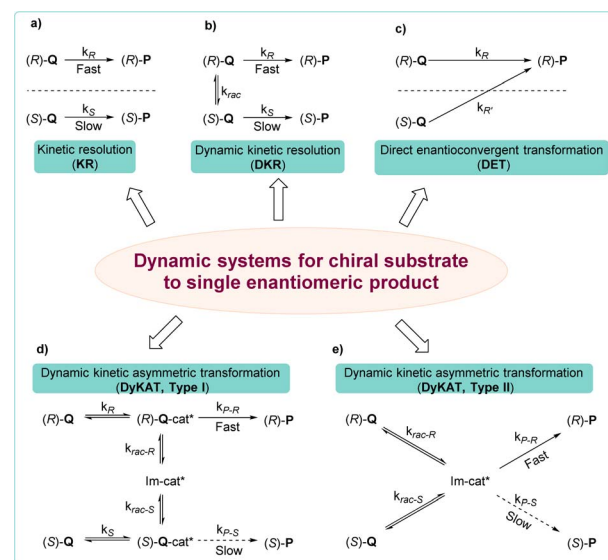
Although the use of stabilized nucleophiles ( $pK_a < 25$ ) in Pd-catalyzed AAS reactions for racemic starting materials is well-established in catalysis and synthesis,<sup>10,41</sup> the application of non-stabilized nucleophiles in Cu-catalyzed reactions remains a significant challenge with racemic starting materials. Notably, there are considerable differences between the reaction

mechanisms of Pd-catalyzed and Cu-catalyzed AAS reactions. In Pd-catalyzed AAS, both enantiomers of the starting materials are converted to their corresponding  $\pi$ -allyl-Pd intermediates, which undergo rapid interconversion with each other. Subsequently, an enantioselective step takes place, leading to the formation of a new stereogenic center (Scheme 1b). On the other hand, Cu-catalyzed AAS is widely recognized to proceed through regiospecific anti-addition, with  $S_N2'$  oxidative addition as the rate-determining step. Unlike in Pd-catalysis, Cu-allyl intermediates lack an efficient pathway for  $\sigma$  to  $\pi$  isomerization (Scheme 1b and c).<sup>34</sup> If reductive elimination occurs rapidly, the  $\pi$ -allyl-Cu species will not form. As a result, reactions using racemic starting materials will yield racemic products in the absence of a dynamic process (Scheme 1c).

## 1.2 Dynamic processes

The development of Cu-catalyzed AAS for prochiral substrates, which has been extensively pursued, mainly relies on the use of organometallic reagents.<sup>31,42–48</sup> The recent trend of using unsaturated hydrocarbons as pro-nucleophiles in borylative or reductive couplings with allylic substrates represents a significant development in this field, facilitating the synthesis of products endowed with enhanced functional groups.<sup>49–54</sup>

Methods involving racemic and *meso* starting materials that undergo dynamic processes to yield single enantiomer products are highly sought after, due to the greater availability of racemic substrates compared to prochiral ones and the more complex chiral induction process in racemic/*meso* substrates.<sup>55</sup> Employing a chiral catalyst allows only one enantiomer of the racemic substrate to selectively engage in the reaction, yielding a product with remarkable enantioselectivity. This typical process is commonly referred to as kinetic resolution (KR).<sup>56–60</sup>



**Scheme 2** Dynamic processes of a racemate in asymmetric reactions: (a) kinetic resolution; (b) dynamic kinetic resolution; (c) direct enantioconvergent transformation; (d) type I dynamic kinetic asymmetric transformation; (e) type II dynamic kinetic asymmetric transformation.



However, this approach limits the yield of the reaction to 50% in order to ensure optimal enantioselectivity of the final product (Scheme 2a). Unlike the classic KR process, parallel kinetic resolution (PKR) introduces a strategy where both enantiomers of a racemate can be converted into different products.

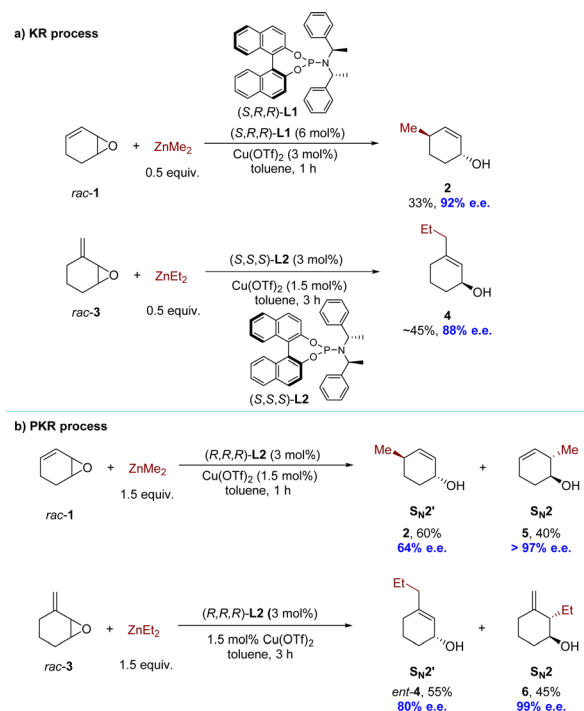
When it comes to the conversion of both enantiomers of a racemate into a single enantiomer, there are typically three approaches: (1) dynamic kinetic resolution (DKR),<sup>61,62</sup> in which the two enantiomers undergo a reversible racemization process before the KR process, which overcomes the 50% maximum yield problem (Scheme 2b); (2) dynamic kinetic asymmetric transformation (DyKAT), in which the equilibration of both enantiomers is facilitated by the presence of a chiral catalyst.<sup>63–65</sup> In type I DyKAT (Scheme 2d), both enantiomers bind to the catalyst and undergo equilibration as intermediates. Conversely, in type II DyKAT (Scheme 2e), the racemate interacts with the chiral catalyst to form a prochiral intermediate **Im-cat\***, resulting in the loss of the stereocenter. These two processes have enabled a diverse range of asymmetric transformations, delivering a fascinating array of chiral building blocks; (3) direct enantioconvergent transformation (DET), in which both enantiomers of the starting material are converted to the same enantiomeric product *via* two distinct mechanistic pathways (Scheme 2c).<sup>66,67</sup> To produce identical enantiomeric products, both pathways must exhibit opposite enantioselectivity, thus necessitating an opposite stereochemical course, which means opposite regioselectivity is essential.

The utilization of these strategies has emerged as a flourishing approach over the past decade in asymmetric catalysis, primarily focusing on the bond-forming reactions for the synthesis of enantioenriched compounds. In this review, we focus on providing a detailed and explicit outline of copper catalyst-mediated dynamic asymmetric catalytic processes in AAS.

## 2. Racemic compounds as starting materials

### 2.1 Kinetic resolution

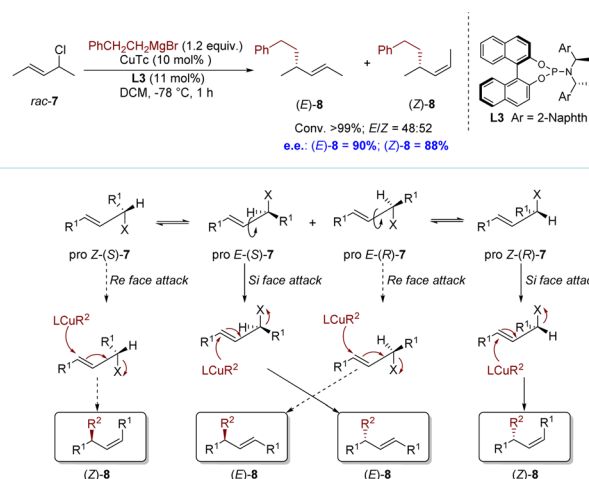
Given the value of Cu-catalyzed AAS with racemic substrates, the Feringa group reported pioneering research in 1998 on the catalytic enantioselective addition of simple organozinc reagents to cycloaliphatic vinyloxiranes.<sup>68–71</sup> Employing a chiral ligand 2,2'-binaphthyl-based phosphorus amidites **L1** and copper(II) triflate  $\text{Cu}(\text{OTf})_2$ , the corresponding allylic alcohol products were obtained *via* an *anti*- $\text{S}_{\text{N}}2'$ -pathway with moderate to high regioselectivity but limited yield (<50%). Using 0.5 equivalents of the nucleophile, the KR of racemic 1,3-cyclohexadiene monoepoxide was achieved, yielding product **2** in 33% yield with 92% enantiomeric excess (e.e.), while recovering the unreacted allylic epoxide **1** with high optical purity. Using ligand **L2** and methylenecycloalkane epoxide **3** as the substrate, the corresponding allylic alcohol **4**, derived from a conjugate addition pathway (*anti*- $\text{S}_{\text{N}}2'$ ), was obtained with excellent regio- and enantioselectivity (88% e.e.) (Scheme 3a). When employing an excess of nucleophiles, these cyclic allylic epoxides underwent the PKR process,<sup>72</sup> wherein the two enantiomers within the substrate reacted with



Scheme 3 Catalytic enantioselective addition to cycloaliphatic vinyloxiranes: (a) KR process; (b) PKR process.

nucleophiles *via* either  $\text{S}_{\text{N}}2$  or  $\text{S}_{\text{N}}2'$  pathways, resulting in distinct products (Scheme 3b). Subsequently, a series of KR or PKR processes of racemic epoxides have been developed.<sup>73–75</sup>

In 2011, the Alexakis group reported an AAS reaction of acyclic allylic chlorides with Grignard reagents (Scheme 4).<sup>76</sup> The conformational flexibility of acyclic substrates, particularly the potential for intramolecular rotation around the carbon-carbon bond, adds an additional layer of complexity to the catalytic processes. This reaction was considered as a stereo-divergent parallel kinetic resolution (SKR) process.<sup>77</sup> Oxidative addition of the pro-*E* conformer of (*S*)-**7** was highly favorable, resulting in the formation of the (*E*)- $\sigma$ -allyl intermediate.

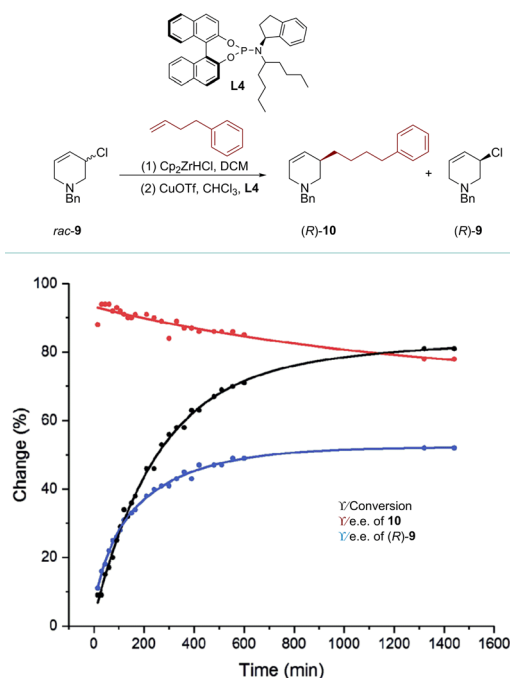


Scheme 4 SKR *via* Cu-catalyzed AAS with acyclic racemic substrates and its plausible reaction mechanism.

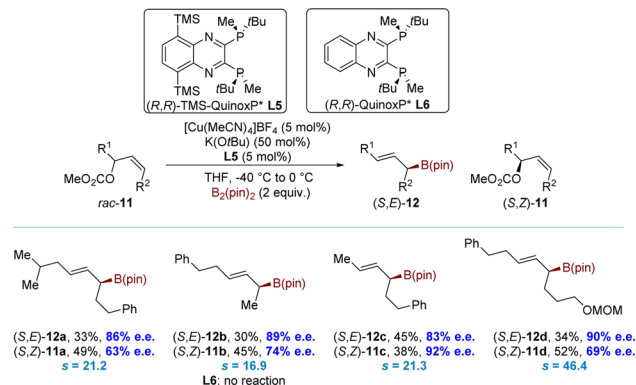


Subsequent reductive elimination, either directly or through the  $\pi$ -allyl complex, would selectively yield the *E* isomer of alkylation product **8**. In stark contrast, an *anti*-attack on the pro-*E* conformer of (*R*)-**7** would involve the olefin being approached from its *Re* face. This possibility would be significantly disfavored; however, the conformational flexibility of an acyclic system allowed rotation around the C3–C4 bond, leading to the formation of the pro-*Z* conformer of the substrate. The latter could then be attacked on its *Si* face, producing the (*Z*)- $\sigma$ -allyl intermediate. This could be followed by the potential formation of a  $\pi$ -allyl complex and ultimately yielding (*Z*)-**8** after reductive elimination. The facial selectivity could be attributed to steric interactions between the chiral ligand and the vinylic methyl group. Interestingly, the Alexakis group also found a slight difference in the reaction rate between the enantiomers of the substrates. Specifically, (*R*)-**7** exhibits higher reactivity towards nucleophilic reagents. However, it is worth noting that the discrepancy in rates between enantiomers is relatively minimal. Consequently, it is currently a challenge to obtain a single (*Z*)-**8** using this method (up to *E/Z* = 43 : 57).

Recently, the Fletcher group reported a rare kinetic resolution of allylic chlorides, forming piperidine-based allylic chlorides with high e.e. This AAS process was achieved using Zr-nucleophiles and a copper catalyst.<sup>78</sup> The reaction progress of 1-benzyl-3-chloro-1,2,3,6-tetrahydropyridine (*rac*-**9**) with 4-phenyl-1-butene was monitored over time (Scheme 5). After 30 minutes at  $-10^\circ\text{C}$ , the conversion reached 16%, resulting in the formation of product **10** with a high e.e. of 94%. However, as the less reactive enantiomer of *rac*-**9** was gradually consumed during the reaction, the e.e. of compound **10** decreased by



Scheme 5 KR of *rac*-**9** using a copper catalyst and an alkyl zirconium reagent (reproduced from ref. 78 with permission from The Royal Society of Chemistry).



Scheme 6 KR of *rac*-**11** using a copper catalyst and bis(pinacolato)diboron  $[\text{B}_2(\text{pin})_2]$ .

approximately 15%. On the other hand, the e.e. of compound *rac*-**9** increased from 0% to 80% after continuously reacting for about 22 hours. Under optimized conditions, product (*R*)-**9** was obtained in 30% yield with up to 99% e.e. Furthermore, experiments involving D-labelled chloro-tetrahydropyridine and density functional theory (DFT) calculations were conducted to investigate the mechanistic pathways of this process. These studies revealed that the alkylation of (*R*)-**9** was kinetically disfavored compared to (*S*)-**9**, primarily *via syn-S<sub>N</sub>2'* pathways.

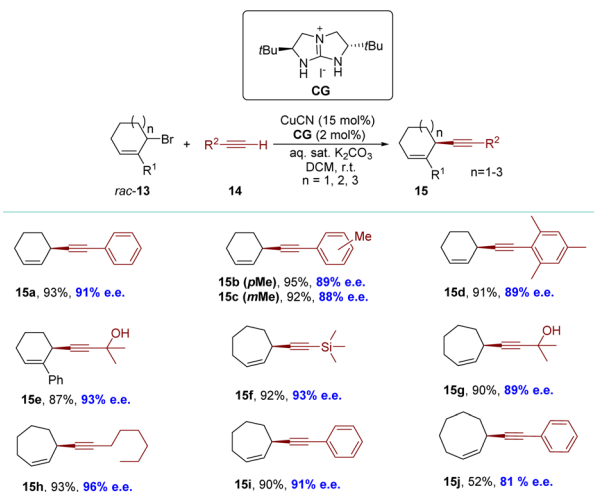
More recently, the Ito group developed a novel series of high-performance  $\text{C}_2$ -symmetrical chiral bisphosphine ligands.<sup>79</sup> These ligands were modified by incorporating silyl groups into the (*R,R*)-QuinoxP\* ligand backbone. Late on, the group successfully executed a borylative kinetic resolution of acyclic allyl electrophiles using the modified ligand (**L5**) (Scheme 6). This ligand showed remarkable selectivity and reactivity in the borylative kinetic resolution of *rac*-**11** at low temperatures, achieving *s* values up to 46.4. The allyl carbonates *rac*-**11** were efficiently converted into the corresponding allyl boronates (*S,E*)-**12** with high selectivity under optimized conditions. Meanwhile, the allyl carbonates (*S,Z*)-**11** were recovered with moderate to high enantioselectivity. The introduction of silyl groups on the ligand proved to be crucial for this process. In contrast, the unmodified ligand (*R,R*)-QuinoxP\* (**L6**) demonstrated an extremely low conversion of *rac*-**11**.

## 2.2 Dynamic kinetic resolution

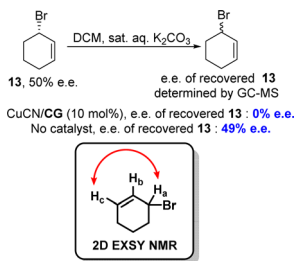
A more universally applicable approach involves the development of dynamic processes, wherein the initial substance undergoes racemization either during the reaction or is recovered post-reaction, racemized, and reintroduced into the reaction conditions. This effectively overcomes the limitation of a maximum yield of 50% in the KR process. In 2018, the Tan group employed functionalized terminal alkynes as pro-nucleophiles to synthesize cyclic 1,4-enynes with 6-, 7- and 8-membered rings, achieving high yields and excellent enantioselectivities under mild reaction conditions (Scheme 7).<sup>80</sup> This system was compatible with various terminal alkynes and cyclic allylic bromides. The identification of catalytic intermediates,







Scheme 7 Guanidine-copper catalyzed enantioselective allylic alkylation of racemic bromides.



Scheme 8 Racemization of enantioenriched allylic bromide 10.

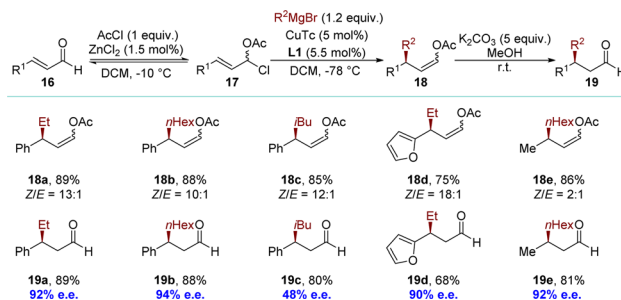
such as guanidinium cuprate ion pairs and a copper-alkynide complex, was achieved through the utilization of cold-spray ionization mass spectrometry (CSI-MS) and X-ray crystallography (XRD). A direct correlation between the enantiopurity of the catalyst and the reaction product suggests the presence of a copper complex with a singular guanidine ligand during the enantio-determining step.

To elucidate the stereo-dynamic process of the reaction, the authors conducted a two-dimensional exchange spectroscopy nuclear magnetic resonance (2D EXSY NMR) analysis to investigate the potential ligand-dependent *syn*-S<sub>N</sub>2' reaction between allylic bromide and allylic cyanide. During the initial optimization of the reaction conditions, they introduced the corresponding guanidine (free base) of CG into the reaction mixture (in the absence of iodide) and observed a similar reaction profile, thereby ruling out any involvement of allylic iodide as an intermediate in racemization. Additionally, rapid racemization of allylic bromide occurred when enantioenriched 13 (50% e.e.) was employed with the catalytic system. By employing 2D EXSY NMR spectroscopy, they detected a chemical exchange between H<sub>a</sub>(Br) and H<sub>c</sub>(Br) protons in 13 in the presence of a guanidine-copper complex (Scheme 8). These findings suggest that the presence of the guanidine-copper complex significantly enhanced racemization rates for allylic bromides, likely through *syn*-S<sub>N</sub>2' isomerization which played a crucial role in successful dynamic kinetic resolution.

### 2.3 Dynamic kinetic asymmetric transformation

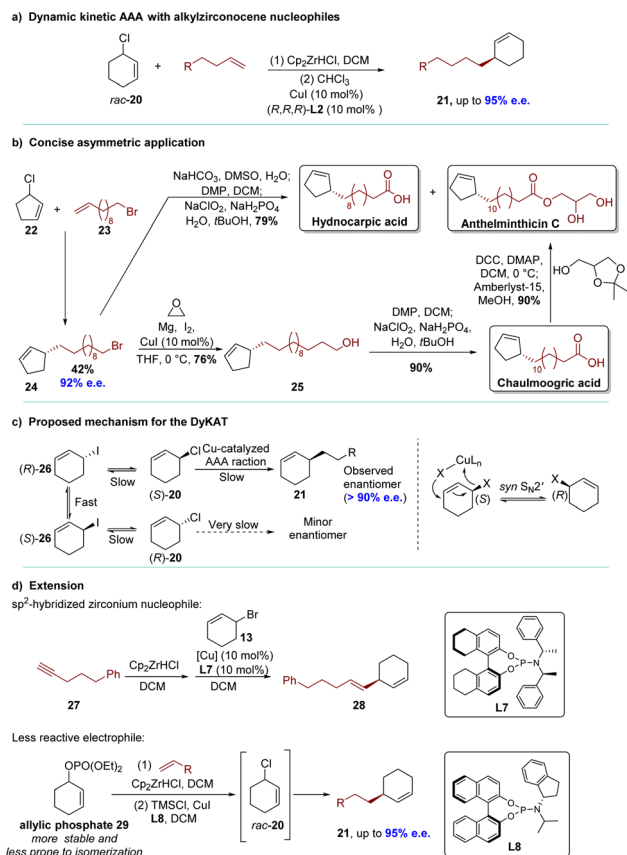
The concept of dynamic kinetic asymmetric transformation (DyKAT) in allylic substitution was introduced by Trost at the end of the 90s, representing one of the most efficient methodologies for converting a racemic substrate into an enantioenriched product.<sup>81,82</sup> Although copper exhibits high catalytic efficiency in promoting the formation of enantioselective allylic C-C bonds using non-stabilized nucleophiles, reports on copper-catalyzed DyKAT were absent until 2010. The Feringa group pioneered the development of a catalytic asymmetric synthesis for chiral enol acetates (Scheme 9).<sup>83</sup> The method includes the *in situ* conversion of  $\alpha,\beta$ -unsaturated aldehydes 16 into  $\alpha$ -chloroallylic acetates 17, followed by regio- and enantioselective allylic alkylation of the  $\alpha$ -chloroallylic acetates 17 to yield products (Z)-18. This innovative method provides access to highly desirable  $\beta$ -substituted aldehydes 19. The process might operate *via* a DyKAT process, where one enantiomer of the  $\alpha$ -chloroallylic acetates 17 reacts more rapidly than the other with the chiral organocopper key intermediate. The equilibrium between the  $\alpha$ -chloroallylic acetates 17 and the  $\alpha,\beta$ -aldehydes 16 likely serves as the racemization mechanism.

In 2015, the Fletcher group reported a remarkable copper-catalyzed DyKAT process involving the asymmetric allylic alkylation of racemic cyclic allylic chlorides with alkyl zirconocenes.<sup>84–86</sup> This convenient procedure enabled the synthesis of highly enantioenriched products at room temperature (Scheme 10a). The investigation commenced with an examination of the interaction between racemic 3-substituted cyclohexenes and alkyl zirconium species, which were generated *in situ* from terminal alkenes and Schwartz's reagent (Cp<sub>2</sub>ZrHCl) (up to 95% e.e.). The study demonstrated the rapid accessibility of crucial structural motifs, as evidenced by the successful asymmetric syntheses of biologically active cyclopentene-containing natural products (hydnocarpic acid, chaulmoogric acid and anthelminticin C) (Scheme 10b). The scope of nucleophilic reagents was significantly expanded by this research, as it demonstrated compatibility with halogens, alkynes, aromatic rings, ethers, protected alcohols, and the trifluoromethyl group. However, the generation of alkyl zirconium species in this reaction requires the use of terminal alkenes and Schwartz's reagent. The applicability of this method for constructing chiral products containing methyl or



Scheme 9 Copper-catalyzed synthesis of chiral enol acetates and aldehydes *via* allylic alkylation of *in situ* formed  $\alpha$ -chloroallylic acetates.





**Scheme 10** Addition of alkyl zirconium reagents to racemic cyclic allylic chlorides via DyKAT: (a) dynamic kinetic AAA with alkylzirconocene nucleophiles; (b) concise asymmetric application; (c) proposed mechanism for the DyKAT; (d) extension.

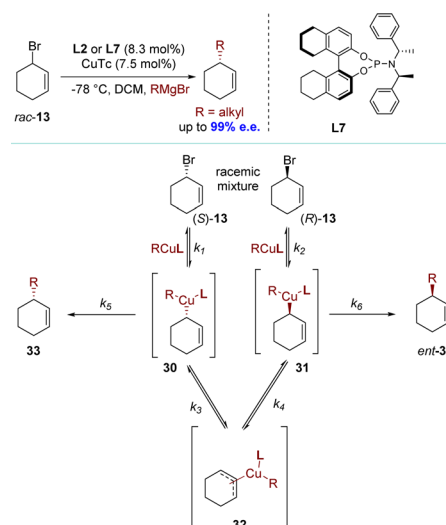
secondary alkyl groups is somehow limited by this stipulation. Mechanistic studies suggested that this DyKAT occurred through a rapidly interconverting intermediate, which racemized the substrate by the I anion (Scheme 10c). The racemization of **20**, probably through *syn*-S<sub>N</sub>2' displacement,<sup>87</sup> and the selective AAS of (*S*)-**20** resulted in products with high e.e. *In situ* <sup>1</sup>H-NMR spectroscopy was employed to gather kinetic data, which were then fitted to a model. This data, in conjunction with EXSY and diffusion-ordered spectroscopy (DOSY) experiments, suggested that the catalyst evolves over time to become more efficient and more enantioselective. The initial catalyst is presumed to be dimeric, such as Cu<sub>2</sub>I<sub>2</sub>L<sub>2</sub>. However, as the reaction progressed and the Cl anion was released from the substrate, a more selective catalytic complex containing both I and Cl anions, such as Cu<sub>2</sub>IClL<sub>2</sub>, was formed. This evolved catalyst exhibited a threefold increase in reactivity compared to the original catalyst. The structure–activity relationships demonstrated that, in specific cases, remarkable stereochemical control could be achieved by converting racemic mixtures of diastereomers into a single diastereoisomer product with high e.e. After that, the same group successfully applied this method to alkenyl zirconocene reagents, building upon their previous work with well-tuned DYKAT and alkyl zirconocene nucleophiles.<sup>88</sup> This elegant demonstration showcases the use of sp<sup>2</sup>-

hybridized nucleophiles in DYKAT (Scheme 10d). Furthermore, this asymmetric allylic alkylation (AAA) system was developed utilizing racemic allylic phosphates and a novel ligand **L8**.<sup>86</sup> This transformation was achieved by utilizing allylic chloride **20**, which was formed *in situ* through the action of TMSCl or from an adventitious Cl anion generated from reaction components (Scheme 10d). The ability to rapidly generate isomerizing allylic halide species *in situ* from these phosphates **29** is likely to have significant utility in chemistry.

## 2.4 Direct enantioconvergent transformation

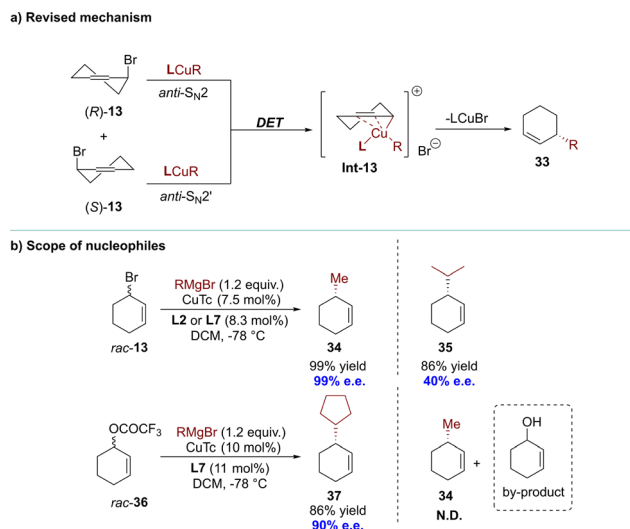
Over the past decade, significant attention has been paid to the synthesis of enantiomerically enriched molecules through DET processes. This process lacks any observable dynamic or reversible characteristics in terms of organic stereogenicity, distinguishing it from conventional DKR and DyKAT processes.

In 2009, the Alexakis group reported the alkylation of racemic cyclohex-1-enyl-3-bromide **13**. This reaction employed copper(i) thiophene-2-carboxylate (CuTc) with **L2** or **L7**, achieving high efficiency (up to 99% e.e.) with primary alkyl Grignard reagents (Scheme 11).<sup>89,90</sup> Based on the experimental results, the authors proposed a plausible reaction mechanism (Scheme 11). The initial step involved ionizing the substrate through metal insertion at the allylic terminus (oxidative addition), while the final step, reductive elimination, led to a mixture of products **33** and *ent*-**33**. During these two steps, an equilibrium was established between  $\sigma$ -allyl species **30** and **31**, derived from ionization of (*S*)-**13** and (*R*)-**13** respectively, *via meso*- $\pi$ -allyl complex **32**. Allylic bromides exhibited high reactivity and Cu(III) intermediates presumably underwent equilibration *via*  $\pi$ -allyl intermediates similar to type **32**. Consequently, the rate-determining step shifted towards reductive elimination ( $k_1, k_2, k_3, k_4 \gg k_5, k_6$ ). After conducting control experiments to rule out the hypothesis of KR, it was determined that enantio-discrimination resulted from differences in reductive elimination rates, which disrupted



**Scheme 11** Alexakis' work and the proposed mechanism for the DyKAT.





**Scheme 12** (a) Revised reaction mechanism and the scope of sterically hindered nucleophiles; (b) scope of nucleophiles.

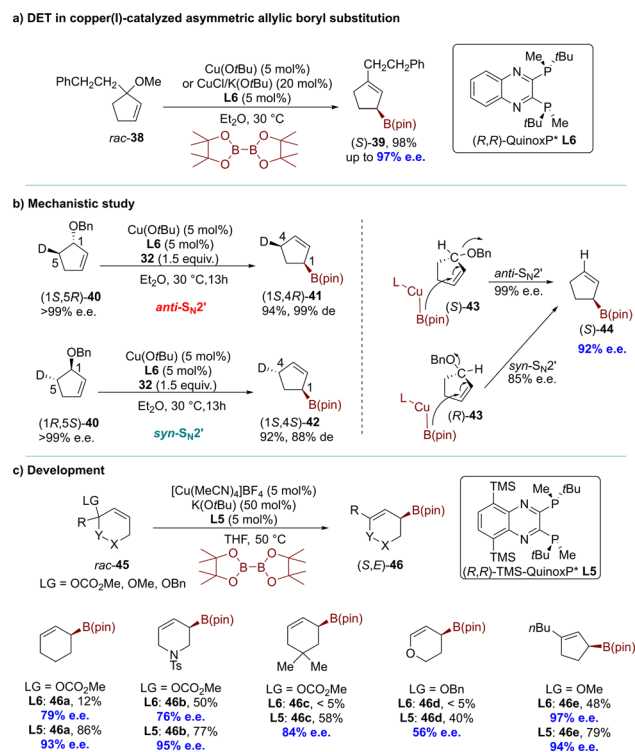
intermediate equilibration and favored the formation of products with higher elimination rates.

Notably, three years later, the Alexakis group found through DFT calculations that the rate of the oxidative addition step was much lower than the rate of the reductive elimination step ( $k_1$ ,  $k_2 \ll k_5$ ,  $k_6$ ), which was inconsistent with previous assumptions.<sup>91</sup> The same group proposed a revised mechanistic route, highlighting the divergent reactivities of both enantiomers of the substrate (Scheme 12a).<sup>91</sup> Indeed, (*R*)-13 underwent an *anti*- $S_N2'$  oxidative addition, while its antipode reacted in an *anti*- $S_N2$  manner. This regiodivergent oxidative addition facilitated the formation of a common Cu(III) intermediate, characterized as a cationic  $\sigma$ - $\pi$ -enyl copper complex, referred to as **Int-13**. No equilibrations were expected from this key intermediate, and a rapid reductive elimination led to the desired product (*R*)-33. The absence of any resolving step and the distinct mechanistic pathways for each enantiomer of 13 established this process as a direct enantioconvergent transformation (DET).

Additionally, the same research group reported further enhancements to the process and expanded the scope of the nucleophiles.<sup>91</sup> These advancements included the utilization of both primary alkyl and sterically hindered secondary alkyl Grignard reagents, which effectively demonstrated the versatility of this methodology. However, this catalytic system proved incompatible with Grignard reagents that varied in activity and steric hindrance (Scheme 12b). The efficacy of the allylic bromide substrate improved when employing highly active nucleophiles with less steric hindrance (Me, Et, and *n*Bu); however, its effectiveness decreased with the use of sterically hindered nucleophiles.<sup>89,90</sup> On the other hand, the allylic ester substrate outperformed allylic bromide when employing sterically hindered cyclic nucleophiles; however, no product was observed in the presence of a less active methyl Grignard reagent, resulting in only hydrolysis by-products.<sup>91</sup>

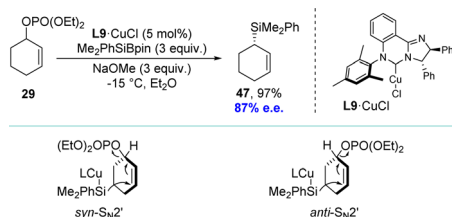
In 2010, the Ito group introduced a DET process promoted by an artificial catalyst.<sup>67</sup> The copper(I)-catalyzed AAS of a racemic

allylic ether resulted in the formation of a single enantiomer of a chiral  $\alpha$ -allylboronate with complete conversion and high enantioselectivity (up to 98% e.e.). One enantiomer of the substrate underwent an *anti*- $S_N2'$ -type reaction, while the other reacted *via* a *syn*- $S_N2'$  pathway (Scheme 13a). These products, which could not be synthesized using dynamic procedures, have been utilized for constructing all-carbon quaternary stereocenters. The reaction of *rac*-38 was initially conducted with  $B_2(\text{pin})_2$  in the presence of Cu(*Ot*Bu) and a chiral phosphine ligand (*R,R*)-QuinoxP\* (**L6**) in diethyl ether at 30 °C. Complete conversion of *rac*-38 was achieved within 24 hours in a  $S_N2'$  manner, yielding the corresponding allyl boronate (*S*)-39 in high yield (98%) with excellent enantioselectivity (up to 97% e.e.). Further experiments using deuterated substrates clearly demonstrated that the two enantiomers underwent distinct pathways, namely *anti*- $S_N2'$  and *syn*- $S_N2'$ , while the chiral centers adjacent to the deuteride remained unchanged. Consequently, this resulted in the formation of two diastereomeric products from each enantiomer. The experimental results could be adequately explained by assuming a direct enantioconvergent reaction. When (*R,R*)-QuinoxP\* (**L6**) was used as the ligand in the AAS of (*S*)-43, the nucleophilic attack occurred on the opposite face of the carbon-carbon double bond relative to the leaving group, resulting in the formation of (*S*)-44 through an *anti*- $S_N2'$ -type pathway with 99% e.e. In contrast, when approaching (*R*)-43, the same borylcopper(I) intermediate approached from the same side as the leaving group, leading to



**Scheme 13** Copper(I)-catalyzed asymmetric allylic boryl substitution *via* DET and its plausible reaction mechanism: (a) DET in copper(I)-catalyzed asymmetric allylic boryl substitution; (b) mechanistic study; (c) development.





Scheme 14 Copper(I)-catalyzed asymmetric allylic silylation *via* DET and its plausible reaction mechanism.

the formation of (*S*)-**44** through a *syn*-S<sub>N</sub>2'-type reaction with 85% e.e (Scheme 13b). A decade later, the Ito group modified (*R,R*)-QuinoxP\* (**L6**) by introducing the silyl moieties into the ligand's backbone, resulting in (*R,R*)-5,8-TMS-QuinoxP\* (**L5**).<sup>79</sup> The introduction of silyl moieties significantly improved the reactivity and enantioselectivity in the direct enantioconvergent borylation of substrates. The borylation products, including heterocyclic structures, were obtained with higher yield and excellent enantioselectivity, surpassing the results from using (*R,R*)-QuinoxP\* (**L6**) (Scheme 13c).

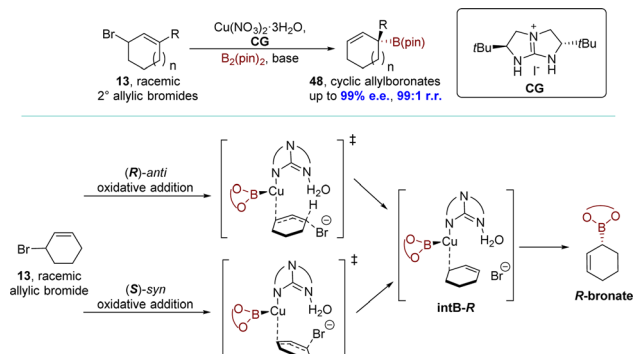
Inspired by the work of the Alexakis and Ito groups, the Oestreich group developed a copper(I)-catalyzed asymmetric allylic silylation of racemic cyclic phosphates using Me<sub>2</sub>-PhSiBpin as the silicon pronucleophile (Scheme 14).<sup>92</sup> The group successfully converted racemic cyclic allylic phosphate **29** into highly enantioenriched cyclic allylic silane **47** in near-quantitative yield. The NHC-copper(I) chloride complex L9·CuCl was transformed into the active catalyst L9·CuOMe *via* ligand metathesis with sodium methoxide, facilitating this reaction. Observations from matched and mismatched substrate/catalyst combinations revealed that both enantiomers undergo S<sub>N</sub>2' reactions, each with opposite diastereofacial selectivity. Consequently, the enantiomeric allylic phosphates lead to the identical allylic silane *via* two separate reaction mechanisms, defining it as a DET process.

Given the profitability of the efficient dynamic kinetic copper-catalyzed AAS reaction with a chiral bicyclic guanidine, the Tan group reported a monodentate guanidine-copper(I) complex catalyzed S<sub>N</sub>2' borylation process in 2019. This transformation proceeded through a unique DET mechanism. The allyl boronates **48** were obtained with exceptional

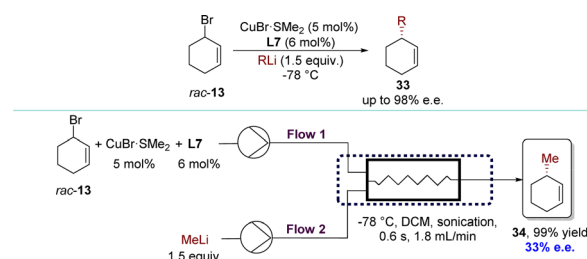
regioselectivities (up to 99 : 1 r.r.) and enantioselectivities (up to 99% e.e.). This allowed their subsequent transformation into a wide range of functionalized secondary and tertiary allylic compounds while maintaining their optical purity (Scheme 15).<sup>93</sup> The DFT calculations indicated that the reaction follows the DET mechanism, in which the (*R*)- and (*S*)-enantiomers of allylic bromide **13** undergo kinetically competitive pathways: (*R*)-*anti* oxidative addition and (*S*)-*syn* oxidative addition respectively. These pathways led to the formation of a common intermediate **intB-R** without involving conventional resolving steps. Subsequently, a barrierless B–C bond formation occurred, generating the stereochemically preferred (*R*)-boronate.

In 2022, the Chen group developed a novel Cu-catalyzed AAA process that enabled the enantioconvergent transformation of various racemic cyclic allylic bromides using organolithium reagents, giving the product in high yields with enantioselectivities (Scheme 16).<sup>94</sup> Utilizing CuBr·SMe<sub>2</sub> and phosphoramidite ligand **L7** facilitated convenient access to optically pure cycloalkene derivatives. Furthermore, the catalytic enantioselective allylic alkylation processes have been successfully adapted to continuous flow techniques,<sup>95–100</sup> but only with 33% e.e. The difference in the contact mode between batch and flow reactions primarily led to a decrease in enantioselectivities. Typically, in batch reactions, organometallic reagents were introduced dropwise over an extended period into the substrate solution to avert side reactions. However, in flow reactions, substrates and organometallic reagents were mixed simultaneously. As a result, highly active allylic bromides resulted in uncatalyzed reactions or reacted with “ate” and “aggregated” copper species<sup>91</sup> which were produced upon the exposure of the chiral catalyst to an excess of organometallic reagents.

Recently, the same research group has updated this highly efficient AAA reaction by incorporating racemic inert cyclic allylic ethers in combination with BF<sub>3</sub>·OEt<sub>2</sub> and a Cu complex (Scheme 17).<sup>101</sup> This catalytic system demonstrated general effectiveness for challenging, sterically hindered Grignard reagents, accommodating both primary and secondary alkyl groups (Scheme 17a). For mechanistic insight, it is possible that the substrates underwent a similar *in situ* conversion process as observed by the Fletcher group,<sup>86</sup> where racemic **13** was formed from *rac*-**49** in the presence of BF<sub>3</sub>·OEt<sub>2</sub> and the Br anion. Subsequently, the resulting racemic **13** might have undergone the same DET process to form the identical intermediate **Int-13**



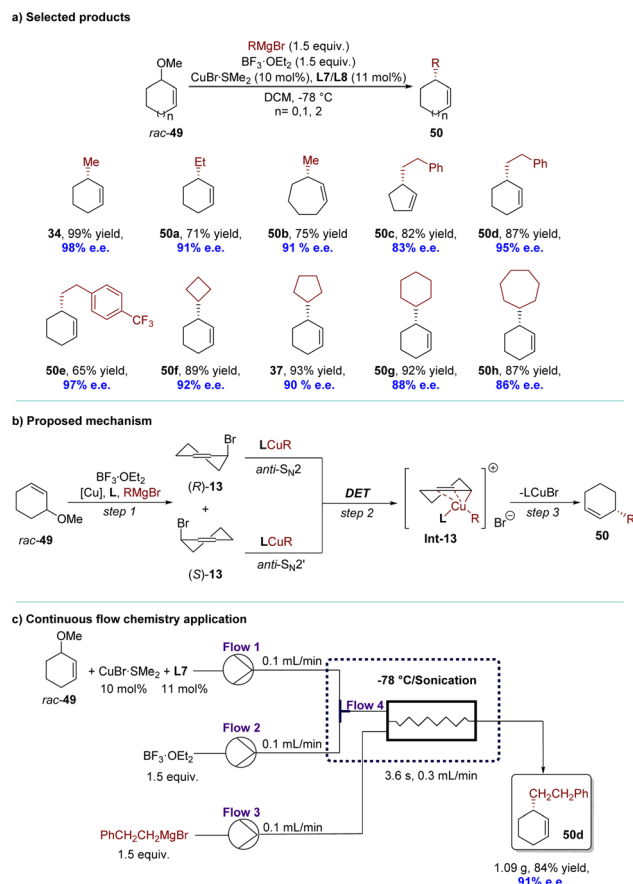
Scheme 15 Guanidine-copper complex catalyzed allylic borylation *via* DET.



Scheme 16 Organolithium reagents in Cu-catalyzed AAA reactions with racemic cyclic substrates *via* DET.





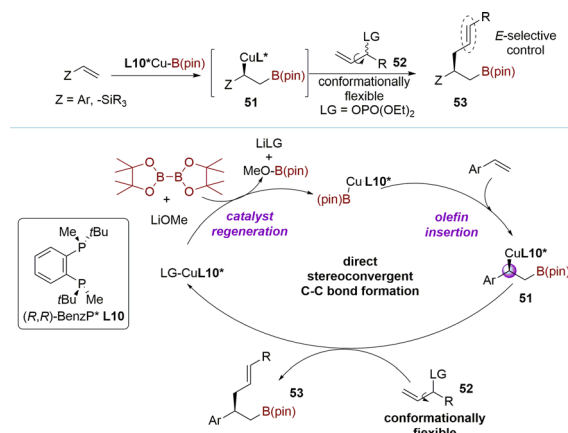


**Scheme 17** Cu-catalyzed AAA of racemic inert cyclic allylic ethers via DET: (a) selected products; (b) proposed mechanism; (c) continuous flow chemistry application.

with Grignard reagents as reported by the Alexakis group.<sup>91</sup> Finally, **Int-13** underwent reductive elimination to yield the desired product **50** with high efficiency and enantioselectivity (Scheme 17b). The method was successfully applied under continuous flow conditions, demonstrating excellent yield and enantioselectivity within a short residence time. Remarkably, benefitting from the *in situ* conversion strategy, the allylic bromide generated *in situ* from allylic ethers would react with privileged copper species rapidly, avoiding most of the side reactions under flow conditions. The catalytic system exhibited uninterrupted operation for over 700 minutes without any loss of yield or enantioselectivity, resulting in the production of 1.09 grams of product **50d** (84% yield, 91% e.e.) (Scheme 17c).

## 2.5 Miscellaneous

The kinetic process is not only applied in constructing chiral centers, but also in controlling the *Z/E* selectivity of reactions. In 2020, the Yun group described the copper-catalyzed stereoconvergent allylation of chiral *sp*<sup>3</sup>-hybridized carbon nucleophiles using a racemic mixture of acyclic secondary allylic phosphates (Scheme 18).<sup>102</sup> The tandem coupling reaction of vinylarenes, **B<sub>2</sub>(pin)<sub>2</sub>**, and racemic allylic phosphates **52** catalyzed by a copper–ligand **L10** complex, led to the formation of



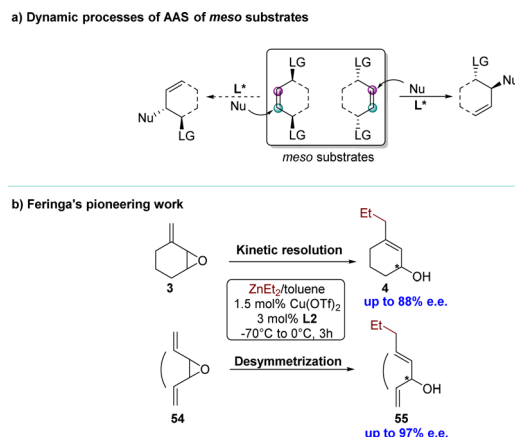
**Scheme 18** Allylation of chiral alkyl-copper nucleophiles with racemic allylic phosphates via DET.

chiral alkylboronates possessing an (*E*)-alkenyl moiety. This transformation proceeded through a direct stereoconvergent allylic coupling, generating a new C(*sp*<sup>3</sup>)-stereogenic center. The insertion of a vinyl arene into a chiral ligand-bound copper-boryl complex resulted in the formation of enantiomerically enriched  $\beta$ -boryl benzyl copper species **51**. This was followed by direct stereoconvergent C–C bond formation between **51** and the racemic secondary allylic electrophile **52**, leading to the desired coupling product **53**. Finally, regeneration of the **L10**\*Cu-Bpin species completed the catalytic cycle. This stereoconvergent transformation process, similar to the DET process, involves converting both enantiomers into an (*E*)-olefin, with the homoallylic chiral center being established during the borylcupration step.

## 3. Meso-compounds as starting materials

Next to the presence of racemic substrates, *meso* compounds constitute a distinct and significant class of substrates containing chiral factors in asymmetric organic reactions.<sup>103</sup> Over the past two decades, the desymmetrization strategy for *meso* compounds has become a crucial, refined, and powerful method in the realm of asymmetric synthesis.<sup>104–108</sup> Notably, the Cu-catalyzed AAS has been extensively utilized in desymmetrization processes to synthesize enantiomerically enriched products, often serving as a strategic approach for accessing natural compounds. The typical dynamic process of a Cu-catalyzed AAS reaction for *meso* substrates can be described as follows: the nucleophile attacks one of the enantiotopic faces of the substrate under the induction of ligands, resulting in an enantiopure product (Scheme 19a). The pioneering work was reported by the Feringa group in 2000 (Scheme 19b).<sup>69</sup> Encouraged by preliminary results from the kinetic resolution protocol with methylenecycloalkane epoxide **3**, they explored the possibility of incorporating dialkylzinc reagents into the enantiotopic faces of a symmetrical *meso* epoxide **54**, thereby circumventing the associated inherent limitations of a kinetic

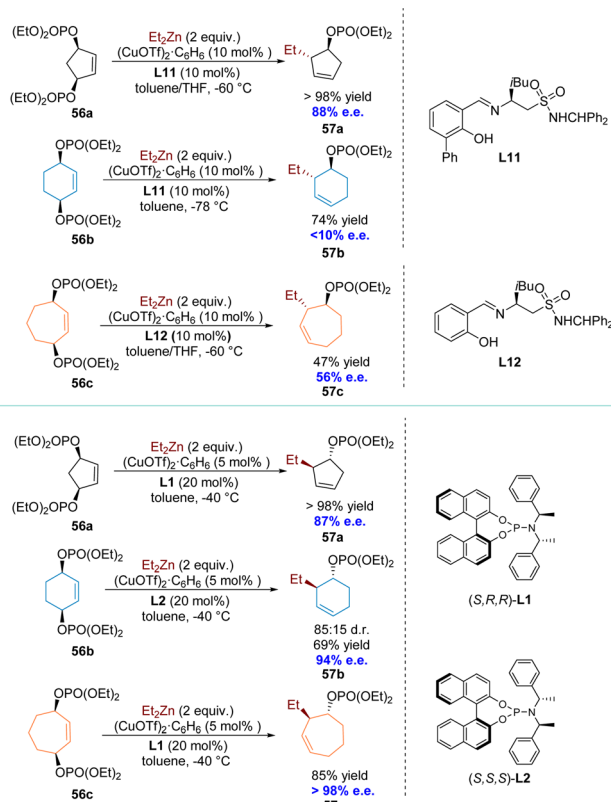




Scheme 19 (a) Dynamic processes of AAS of *meso* substrates (b) Feringa's pioneering work.

resolution process. The first reported catalytic desymmetrization protocol for Cu-catalyzed AAS, using novel symmetrical vinyloxiranes, was disclosed.

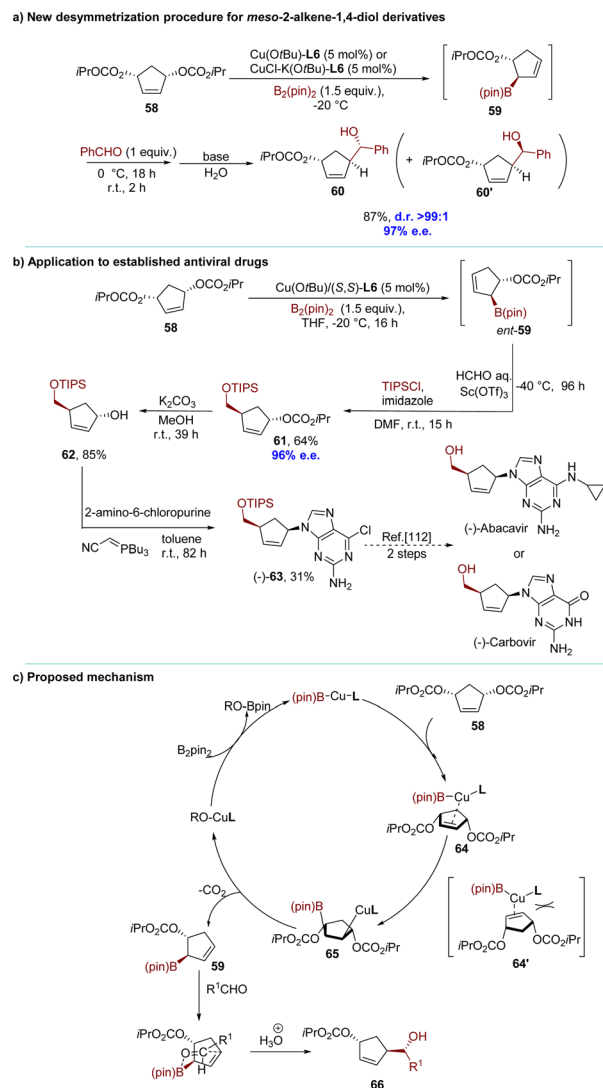
In 2003, the Gennari group introduced a novel highly regio-, diastereo-, and enantioselective desymmetrization of *meso*, cyclic allylic bisdiethylphosphates. This method employs organozinc reagents and is catalyzed by copper(i) complexes of chiral Schiff base ligands (**L11**, **L12**) (Scheme 20).<sup>109</sup> For 5-membered ring substrates, the AAS reaction proceeded with



Scheme 20 Desymmetrisation of *meso* cyclic allylic bis(diethyl phosphates) with organozinc reagents.

high yields and predominantly exhibited *anti*-S<sub>N</sub>2' selectivity, achieving an e.e. of 88%. Unfortunately, the applicability of this reaction to substrates with larger ring sizes proved to be unsuccessful.<sup>110</sup> To address this issue, the same group opted to employ phosphoramidite ligands (**L1** and **L2**) and, pleasingly, achieved an e.e. up to 94% for the 6-membered ring product **57b** and predominantly one enantiomer (e.e. > 98%) for the 7-membered ring product **57c**.

The desymmetrization reactions of *meso* compounds through enantioselective catalysis have emerged as a robust strategy for the synthesis of chiral molecules with multiple stereocenters, which garners significant attention. In 2010, the Ito group reported a remarkable desymmetrization protocol through the enantioselective synthesis of allyl boronates catalyzed by copper(i) (Scheme 21).<sup>111</sup> The reaction of the carbonate derivative of *meso*-diol **58** and B<sub>2</sub>(pin)<sub>2</sub>, catalyzed by Cu(OtBu)



Scheme 21 Desymmetrization by copper(i)-catalyzed asymmetric borylation of *meso*-2-alkene-1,4-diol derivatives: (a) new desymmetrization procedure for *meso*-2-alkene-1,4-diol derivatives; (b) application to established antiviral drugs; (c) proposed mechanism.

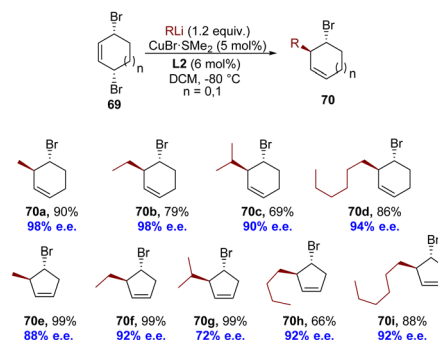


and a chiral ligand (*R,R*)-QuinoxP\* **L6** in toluene at  $-20\text{ }^{\circ}\text{C}$ , was completed efficiently within 4 hours. Subsequently, benzaldehyde was added at  $0\text{ }^{\circ}\text{C}$  to afford compound **60** in high yield (87%) with exceptional diastereo- and enantioselectivities ( $>99:1$  d.r., 97% e.e.). The desymmetrization reaction was employed for the efficient asymmetric synthesis of a precursor to an antiviral medication. This process represented a concise formal synthesis of (–)-abacavir or (–)-carbovir in only five steps (Scheme 21b).<sup>112</sup> Coordination of the *meso* substrate with the chiral borylcopper(i) intermediate yielded complex **64**, thereby avoiding the formation of sterically unfavorable **64'**. Subsequent addition of borylcopper(i) across the carbon–carbon double bond generates alkylcopper(i) **65**, which upon elimination produced the formal *anti*- $\text{S}_{\text{N}}2'$  product allyl boronate **59** and copper(i) carbonate. Regeneration of alkoxy copper(i) was achieved upon the release of carbon dioxide from copper carbonate. Carbonyl addition to **59** proceeded *via* a 6-membered transition state, positioning the  $\text{R}^1$  group equatorially, ultimately yielding product **66** after hydrolysis (Scheme 21c).

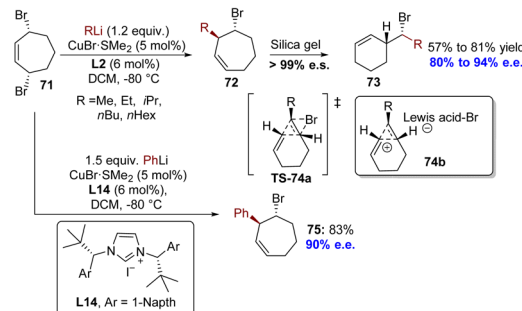
An enantioselective  $\text{S}_{\text{N}}2'$ -type allyl–allyl coupling between allyl boronates and (*Z*)-acyclic/cyclic allylic phosphates was developed by the Sawamura group in 2016 (Scheme 22).<sup>113</sup> The reaction was facilitated by the catalysis of a copper(i) complex utilizing a novel phenol/NHC chiral ligand **L13**, leading to successful application in the desymmetrization of the *meso* cyclic 1,3-diol diphosphate derivative. The reaction exhibited exceptional regioselectivities and moderate enantioselectivities of the  $\text{S}_{\text{N}}2'$ -type, leading to the formation of chiral 1,5-diene derivatives **68** with a tertiary stereogenic center at the allylic position.

A highly regio- and enantioselective desymmetrization of *meso*-1,4-dibromocycloalk-2-enes **69** using AAS with organolithium reagents has been successfully achieved by Feringa's group in 2018, resulting in the formation of bromocycloalkenes with excellent diastereoselectivity and enantioselectivity (Scheme 23).<sup>114</sup> After careful optimization of reaction conditions, the subsequent utilization of 5- or 6-membered substrates led to the successful incorporation of commercially available alkyllithium reagents, resulting in the formation of AAS products **70** with exceptional enantioselectivities (up to  $99:1$  e.r.). When *meso*-3,7-dibromo-cycloheptene **71** was employed in the desymmetrization reaction with an alkyllithium reagent, the

a) Desymmetrization of five and six-membered *meso*-cyclic allylic dibromides



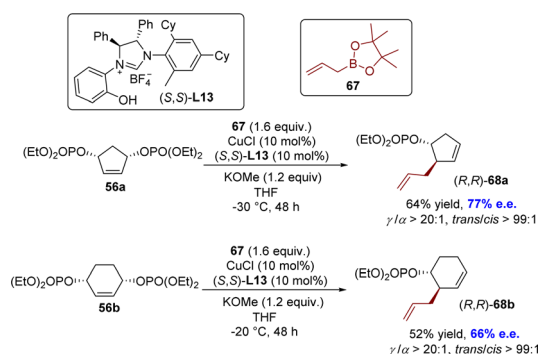
b) Desymmetrization of seven-membered *meso*-cyclic allylic dibromides



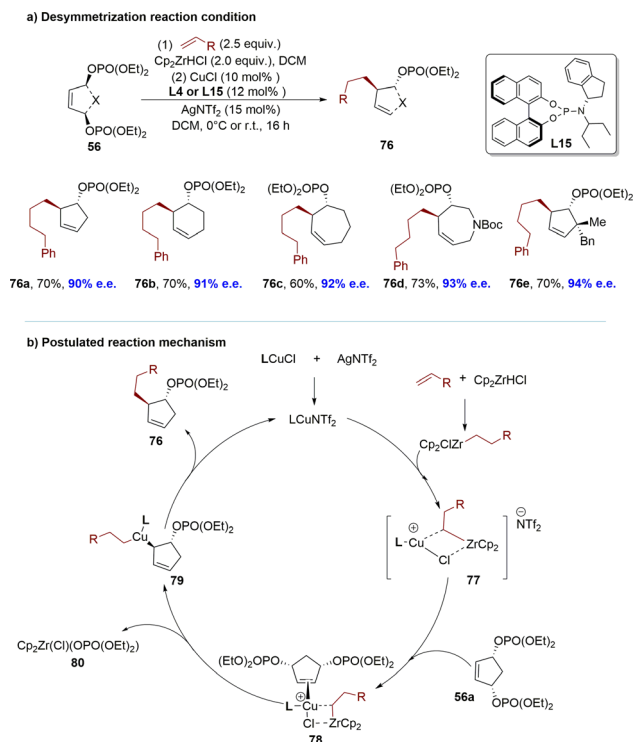
Scheme 23 Desymmetrization of *meso*-dibromocycloalkenes through copper(i)-catalyzed AAS with organolithium reagents: (a) desymmetrization of five and six-membered *meso*-cyclic allylic dibromides; (b) desymmetrization of seven-membered *meso*-cyclic allylic dibromides.

anticipated products **72** were initially obtained with high diastereoselectivity ( $>99:1$  d.r.) and enantioselectivity (80% to 94% e.e.), as determined by NMR and chiral GC analysis (Scheme 23b). However, during the attempted purification of these 7-membered ring products **72** using flash column chromatography on silica gel, only their corresponding cyclohexene analogs **73** were isolated with high stereospecificity. Experimental and theoretical evidence substantiated a rare type I dyotropic rearrangement involving a [1,2]-alkene shift *via* transition state **TS-74a** or a stepwise formal dyotropic rearrangement *via* an ion-pair intermediate **74b**, resulting in regio- and stereospecific ring contraction of bromocycloheptenes.<sup>115</sup> Compared to alkyl groups, phenyl substituents are less susceptible to rearrangement reactions. With the employment of **L14** as the ligand, 7-membered ring product **75** was successfully isolated in 83% yield with excellent enantioselectivity (90% e.e.).

Benefiting from accumulated research in organozirconium reagents, the Fletcher group successfully demonstrated a highly enantioselective Cu-catalyzed desymmetrization of diverse *meso*-cyclic bisphosphates using *in situ* generated hydrozirconated alkene nucleophiles (Scheme 24).<sup>116</sup> To demonstrate the generality of the reaction across various ring sizes, 5-, 6- and 7-membered *meso*-bisphosphates **56** were subjected to desymmetrization using terminal olefins. The reaction accommodates functional groups that are incompatible with numerous conventional organometallic reagents, thereby enabling access

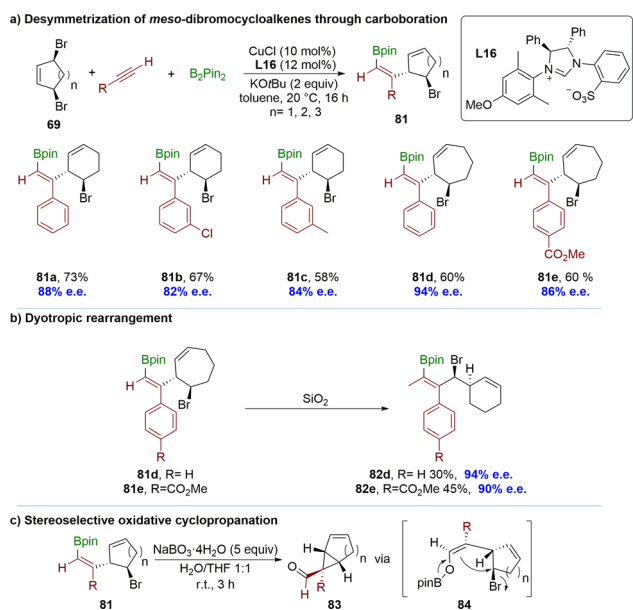


Scheme 22 Desymmetrization by copper(i)-catalyzed enantioselective allyl–allyl coupling.



Scheme 24 Desymmetrization of *meso*-bisphosphates using copper catalysis and alkyl zirconocene nucleophiles: (a) desymmetrization reaction condition; (b) postulated reaction mechanism.

to a wide array of functionalized carbocyclic and heterocyclic structures. The resulting products feature up to three adjacent stereogenic centers, inclusive of quaternary centers and spirocyclic ring systems. Mechanistically, a hybrid species **77** was



Scheme 25 Desymmetrization by copper(i)-catalyzed asymmetric borylative coupling with alkynes: (a) desymmetrization of *meso*-dibromocycloalkenes through carboboration; (b) dyotropic rearrangement; (c) stereoselective oxidative cyclopropanation.

formed between the Cu-phosphoramidite complex and the hydrozirconated alkene, which coordinated with the bisphosphate to form an alkene donor complex **78**. Based on *in situ* NMR spectroscopic studies of reactant and catalyst mixtures, explicit transmetalation from Zr to Cu was not observed. **78** might undergo a stereo determining *anti*-S<sub>N</sub>2'-like process, to generate Cu(III)  $\sigma$ -allyl species **79**, where copper displaced the phosphate. The reductive elimination of intermediate **79** would yield the product **76** and regenerate the Cu-phosphoramidite catalyst (Scheme 24b).

Recently, the Fañanás-Mastral group reported a copper-catalyzed coupling between alkynes, B<sub>2</sub>(pin)<sub>2</sub> and *meso*-dibromocycloalkenes **69** (Scheme 25a).<sup>103</sup> This process enabled the desymmetrization of these *meso* compounds through a net alkyne allylboration reaction using a catalytically generated boron-substituted alkenyl copper intermediate. The method employed a chiral N-heterocyclic carbene (NHC) copper complex for the synthesis of a wide range of chiral cycloalkenes. It is noteworthy that the product contains stereo-defined alkenyl boronate and bromide functionalities, demonstrating excellent regio-, diastereo-, and enantioselectivity. The reaction proceeded excellently with *meso*-dibromocyclopentene, yielding products with exceptional selectivity when employing phenyl acetylene and methyl 4-ethynylbenzoate as pro-nucleophiles. Interestingly, flash column chromatography afforded **82d** and **82e** as the products instead of 7-membered compounds **81d** and **81e**, which could be attributed to a stereospecific ring contraction *via* dyotropic rearrangement (Scheme 25b). The resulting products underwent an oxidative cyclopropanation reaction by treatment with sodium perborate, yielding valuable building blocks **83** for accessing a diverse range of important chiral structures. This cyclopropanation reaction likely involved the oxidation of the alkenyl boronate to form a boron enolate **84**, followed by an intramolecular S<sub>N</sub>2 substitution, where the carbocycle moiety would be positioned opposite to the sizable pinacolboronate (OBpin) unit (Scheme 25c).

## 4. Conclusions

Cu-catalyzed AAS enables the acquisition of enantioenriched building blocks, which are indispensable for the synthesis of bioactive molecules and drugs. Although enantiospecific transformations and additions to prochiral molecules have proven to be valuable tools, the application of racemic or *meso* starting materials remains underdeveloped despite its immense potential. This is largely attributed to the intricate and nuanced interaction between the substrate and the chiral catalyst. This review provides a comprehensive clarification of the terminology associated with dynamic processes in Cu-catalyzed AAS with racemic and *meso* substrates, along with an overview of recent advancements.

Despite the significant progress in this field, there still exist several challenges: (1) while significant advancements have been made in the development of AAS for cyclic racemic and *meso* substrates, acyclic substrates have not been as thoroughly investigated. The conformational flexibility of acyclic substrates, especially the potential for intramolecular rotation





around the carbon–carbon bond, adds an extra layer of complexity to the catalytic processes. Despite the development of several chiral ligands and additives,<sup>76,79</sup> achieving efficient and highly stereoselective allylic substitutions with acyclic racemic substrates remains challenging, with limitations in substrate scope, stereoselectivity and practical applications. (2) Procedures involving unactivated allylic species, such as allylic alcohols, allylic ethers and allylic amines, remain difficult. Notably, their use is advantageous for minimizing the generation of waste by-products and reducing reaction steps, rendering them valuable owing to their inherent stability and prevalence in numerous biologically active compounds;<sup>117</sup> (3) despite the numerous reported examples of enantioselective allylic substitution reactions, significant challenges persist in their development, particularly in syntheses involving quaternary center formation; (4) cooperative bimetallic catalysis involving AAS remains unexplored, despite the growing interest in using second- and third-row transition metals like Pd, Rh, and Ir in bimetallic catalysis. While Cu catalysts are primarily employed as nucleophilic activators in AAS,<sup>118–123</sup> their application in bimetallic systems remains limited; (5) the potent transformation facilitated by Pd, Rh, and Ir has been successfully employed in the total synthesis of numerous natural products. In contrast, the use of Cu catalysis in producing valuable compounds remains relatively limited. Developing effective catalytic systems with greater tolerance for sterically hindered nucleophilic reagents and a broader range of substrates, including acyclic and heterocyclic types, could enhance the potential of Cu catalysis in total synthesis.

Furthermore, mechanistic investigations play a crucial role in advancing this chemistry by enhancing chemists' comprehension of the demands and challenges associated with the dynamic process of racemic or *meso* mixtures. These investigations provide an understanding of current limitations and potential opportunities, inspiring novel strategies and targets. Despite the numerous challenges mentioned above, recent developments in Cu-catalyzed AAS have demonstrated their effective solution. These complexities present an exceptional opportunity for synthetic chemists to apply their expertise to this captivating and crucial field of chemistry.

## Author contributions

J. L. and J. H. performed the literature search, analyzed the published results, and wrote the manuscript. Y. Z., H. Y. and F. C. structured this review. Y. W. and Y. L. provided key advice and supervised the preparation of the text.

## Conflicts of interest

There are no conflicts to declare.

## Acknowledgements

This work was supported by the National Natural Science Foundation of China (No. 22302048; no. 82204231) and Guangdong Basic and Applied Basic Research Foundation (No.

2021A1515110366). We are also grateful to Shenzhen Science and Technology Research Fund No. JSGG20201103153807021; GXWD20220811173736002; KCXFZ20230731094904009 and Shenzhen Key Laboratory of Advanced Functional Carbon Materials Research and Comprehensive Application.

## Notes and references

- G. Zanoni, F. Castronovo, M. Franzini, G. Vidari and E. Giannini, *Chem. Soc. Rev.*, 2003, **32**, 115–129.
- S. Afewerki and A. Córdova, *Chem. Rev.*, 2016, **116**, 13512–13570.
- V. Bhat, E. R. Welin, X. Guo and B. M. Stoltz, *Chem. Rev.*, 2017, **117**, 4528–4561.
- A. H. Hoveyda, Y. Zhou, Y. Shi, M. K. Brown, H. Wu and S. Torker, *Angew. Chem., Int. Ed.*, 2020, **59**, 21304–21359.
- M. Diéguez, *Chiral Ligands: Evolution of Ligand Libraries for Asymmetric Catalysis*, CRC Press, 2021.
- M. Kamlar, M. Urban and J. Veselý, *Chem. Rev.*, 2023, **23**, e202200284.
- B. M. Trost and T. J. Fullerton, *J. Am. Chem. Soc.*, 1973, **95**, 292–294.
- B. M. Trost and P. E. Strege, *J. Am. Chem. Soc.*, 1977, **99**, 1649–1651.
- B. M. Trost and R. C. Bunt, *J. Am. Chem. Soc.*, 1994, **116**, 4089–4090.
- A. H. Cherney, N. T. Kadunce and S. E. Reisman, *Chem. Rev.*, 2015, **115**, 9587–9652.
- V. Hornillos, J.-B. Gualtierotti and B. L. Feringa, in *Progress in Enantioselective Cu(I)-catalyzed Formation of Stereogenic Centers*, ed. S. R. Harutyunyan, Springer International Publishing, Cham, 2016, pp. 1–39.
- L. Süssé and B. M. Stoltz, *Chem. Rev.*, 2021, **121**, 4084–4099.
- S. V. Kumar, A. Yen, M. Lautens and P. J. Guiry, *Chem. Soc. Rev.*, 2021, **50**, 3013–3093.
- T. J. Fulton, Y. E. Du and B. M. Stoltz, in *Catalytic Asymmetric Synthesis*, John Wiley & Sons, Ltd, 2022, pp. 661–704.
- H. Wu, B. Qu, T. Nguyen, J. C. Lorenz, F. Buono and N. Haddad, *Org. Process Res. Dev.*, 2022, **26**, 2281–2310.
- Y. Kobayashi, *Catalysts*, 2023, **13**, 132.
- B. M. Trost and M. L. Crawley, in *Transition Metal Catalyzed Enantioselective Allylic Substitution in Organic Synthesis*, ed. U. Kazmaier, Springer, Berlin, Heidelberg, 2012, pp. 321–340.
- Y. Liu, S.-J. Han, W.-B. Liu and B. M. Stoltz, *Acc. Chem. Res.*, 2015, **48**, 740–751.
- B. W. H. Turnbull and P. A. Evans, *J. Org. Chem.*, 2018, **83**, 11463–11479.
- C. Li, S. S. Ragab, G. Liu and W. Tang, *Nat. Prod. Rep.*, 2020, **37**, 276–292.
- O. Pàmies, J. Margalef, S. Cañellas, J. James, E. Judge, P. J. Guiry, C. Moberg, J.-E. Bäckvall, A. Pfaltz, M. A. Pericàs and M. Diéguez, *Chem. Rev.*, 2021, **121**, 4373–4505.
- M. B. Thoke and Q. Kang, *Synthesis*, 2019, **51**, 2585–2631.



- 23 Q. Cheng, H.-F. Tu, C. Zheng, J.-P. Qu, G. Helmchen and S.-L. You, *Chem. Rev.*, 2019, **119**, 1855–1969.
- 24 F. Dübner and P. Knochel, *Angew. Chem., Int. Ed.*, 1999, **38**, 379–381.
- 25 J. A. Dabrowski, F. Gao and A. H. Hoveyda, *J. Am. Chem. Soc.*, 2011, **133**, 4778–4781.
- 26 R. Shintani, K. Takatsu, M. Takeda and T. Hayashi, *Angew. Chem., Int. Ed.*, 2011, **50**, 8656–8659.
- 27 F. Gao, J. L. Carr and A. H. Hoveyda, *Angew. Chem.*, 2012, **124**, 6717–6721.
- 28 M. Fañanás-Mastral, R. Vitale, M. Pérez and B. L. Feringa, *Chem.–Eur. J.*, 2015, **21**, 4209–4212.
- 29 H. Ohmiya, H. Zhang, S. Shibata, A. Harada and M. Sawamura, *Angew. Chem., Int. Ed.*, 2016, **55**, 4777–4780.
- 30 W. Xiong, G. Xu, X. Yu and W. Tang, *Organometallics*, 2019, **38**, 4003–4013.
- 31 C. I. Jette, Z. J. Tong, R. G. Hadt and B. M. Stoltz, *Angew. Chem., Int. Ed.*, 2020, **59**, 2033–2038.
- 32 S. Niu, Y. Luo, C. Xu, J. Liu, S. Yang and X. Fang, *ACS Catal.*, 2022, **12**, 6840–6850.
- 33 C. A. Falcicola and A. Alexakis, *Eur. J. Org. Chem.*, 2008, **2008**, 3765–3780.
- 34 J.-B. Langlois and A. Alexakis, in *Transition Metal Catalyzed Enantioselective Allylic Substitution in Organic Synthesis*, ed. U. Kazmaier, Springer, Berlin, Heidelberg, 2012, pp. 235–268.
- 35 K. Tissot-Croset, D. Polet and A. Alexakis, *Angew. Chem., Int. Ed.*, 2004, **43**, 2426–2428.
- 36 K. Tissot-Croset and A. Alexakis, *Tetrahedron Lett.*, 2004, **45**, 7375–7378.
- 37 M. Pérez, M. Fañanás-Mastral, P. H. Bos, A. Rudolph, S. R. Harutyunyan and B. L. Feringa, *Nat. Chem.*, 2011, **3**, 377–381.
- 38 V. Hornillos, M. Pérez, M. Fañanás-Mastral and B. L. Feringa, *J. Am. Chem. Soc.*, 2013, **135**, 2140–2143.
- 39 M. S. Manna, S. Y. Yoo, M. Sharique, H. Choi, B. Pudasaini, M.-H. Baik and U. K. Tambar, *Angew. Chem., Int. Ed.*, 2023, **62**, e202304848.
- 40 C. Wang, Y. Wang, X. Jia, J. Huang, H. You and F.-E. Chen, *J. Catal.*, 2023, **425**, 50–56.
- 41 B. M. Trost and D. L. Van Vranken, *Chem. Rev.*, 1996, **96**, 395–422.
- 42 M. Fañanás-Mastral, M. Pérez, P. H. Bos, A. Rudolph, S. R. Harutyunyan and B. L. Feringa, *Angew. Chem., Int. Ed.*, 2012, **51**, 1922–1925.
- 43 C. Jahier-Diallo, M. S. T. Morin, P. Queval, M. Rouen, I. Artur, P. Querard, L. Toupet, C. Crévisy, O. Baslé and M. Mauduit, *Chem.–Eur. J.*, 2015, **21**, 993–997.
- 44 J. A. Dabrowski, F. Haeffner and A. H. Hoveyda, *Angew. Chem.*, 2013, **125**, 7848–7853.
- 45 L. Qin, M. Sharique and U. K. Tambar, *J. Am. Chem. Soc.*, 2019, **141**, 17305–17313.
- 46 Q. Zhang, S.-W. Zhou, C.-Y. Shi and L. Yin, *Angew. Chem., Int. Ed.*, 2021, **60**, 26351–26356.
- 47 S. Guduguntla, J.-B. Gualtierotti, S. S. Goh and B. L. Feringa, *ACS Catal.*, 2016, **6**, 6591–6595.
- 48 X. Li, J. Chen and Q. Song, *Chem. Commun.*, 2024, **60**, 2462–2471.
- 49 F. Meng, K. P. McGrath and A. H. Hoveyda, *Nature*, 2014, **513**, 367–374.
- 50 G. Xu, H. Zhao, B. Fu, A. Cang, G. Zhang, Q. Zhang, T. Xiong and Q. Zhang, *Angew. Chem., Int. Ed.*, 2017, **56**, 13130–13134.
- 51 G. Xu, B. Fu, H. Zhao, Y. Li, G. Zhang, Y. Wang, T. Xiong and Q. Zhang, *Chem. Sci.*, 2019, **10**, 1802–1806.
- 52 E. Rivera-Chao, M. Mitxelena, J. A. Varela and M. Fañanás-Mastral, *Angew. Chem., Int. Ed.*, 2019, **58**, 18230–18234.
- 53 A. Chaves-Pouso, A. M. Álvarez-Constantino and M. Fañanás-Mastral, *Angew. Chem.*, 2022, **134**, e202117696.
- 54 M. Piñeiro-Suárez, A. M. Álvarez-Constantino and M. Fañanás-Mastral, *ACS Catal.*, 2023, **13**, 5578–5583.
- 55 P. Schäfer, M. Sidera, T. Palacin and S. P. Fletcher, *Chem. Commun.*, 2017, **53**, 12499–12511.
- 56 J. Jacques, A. Collet, S. H. Wilen and A. Collet, *Enantiomers, Racemates, and Resolutions*, Wiley, New York, 1981.
- 57 E. L. Eliel and S. H. Wilen, *Stereochemistry of Organic Compounds*, John Wiley & Sons, 1994.
- 58 H. Lorenz and A. Seidel-Morgenstern, *Angew. Chem., Int. Ed.*, 2014, **53**, 1218–1250.
- 59 R. M. Kellogg, *Acc. Chem. Res.*, 2017, **50**, 905–914.
- 60 S. M. Morrow, A. J. Bissette and S. P. Fletcher, *Nat. Nanotechnol.*, 2017, **12**, 410–419.
- 61 F. F. Huerta, A. B. E. Minidis and J.-E. Bäckvall, *Chem. Soc. Rev.*, 2001, **30**, 321–331.
- 62 J. M. Keith, J. F. Larrow and E. N. Jacobsen, *Adv. Synth. Catal.*, 2001, **343**, 5–26.
- 63 B. M. Trost and F. D. Toste, *J. Am. Chem. Soc.*, 1999, **121**, 3543–3544.
- 64 E. Vedejs and M. Jure, *Angew. Chem., Int. Ed.*, 2005, **44**, 3974–4001.
- 65 J. Steinreiber, K. Faber and H. Griengl, *Chem.–Eur. J.*, 2008, **14**, 8060–8072.
- 66 K. Faber, *Chem.–Eur. J.*, 2001, **7**, 5004–5010.
- 67 H. Ito, S. Kunii and M. Sawamura, *Nat. Chem.*, 2010, **2**, 972–976.
- 68 F. Badalassi, P. Crotti, F. Macchia, M. Pineschi, A. Arnold and B. L. Feringa, *Tetrahedron Lett.*, 1998, **39**, 7795–7798.
- 69 F. Bertozzi, P. Crotti, F. Macchia, M. Pineschi, A. Arnold and B. L. Feringa, *Org. Lett.*, 2000, **2**, 933–936.
- 70 F. Bertozzi, P. Crotti, F. Macchia, M. Pineschi and B. L. Feringa, *Angew. Chem., Int. Ed.*, 2001, **40**, 930–932.
- 71 M. Pineschi, *New J. Chem.*, 2004, **28**, 657–665.
- 72 M. Pineschi, F. Del Moro, P. Crotti, V. Di Bussolo and F. Macchia, *J. Org. Chem.*, 2004, **69**, 2099–2105.
- 73 R. Millet and A. Alexakis, *Synlett*, 2007, **2007**, 435–438.
- 74 R. Millet and A. Alexakis, *Synlett*, 2008, **2008**, 1797–1800.
- 75 M. Pineschi, V. D. Bussolo and P. Crotti, *Chirality*, 2011, **23**, 703–710.
- 76 J.-B. Langlois and A. Alexakis, *Angew. Chem., Int. Ed.*, 2011, **50**, 1877–1881.
- 77 L. C. Miller, J. M. Ndungu and R. Sarpong, *Angew. Chem.*, 2009, **121**, 2434–2438.



- 78 S. Karabiyikoglu, A. V. Brethomé, T. Palacin, R. S. Paton and S. P. Fletcher, *Chem. Sci.*, 2020, **11**, 4125–4130.
- 79 H. Iwamoto, Y. Ozawa, Y. Takenouchi, T. Imamoto and H. Ito, *J. Am. Chem. Soc.*, 2021, **143**, 6413–6422.
- 80 X.-Y. Cui, Y. Ge, S. M. Tan, H. Jiang, D. Tan, Y. Lu, R. Lee and C.-H. Tan, *J. Am. Chem. Soc.*, 2018, **140**, 8448–8455.
- 81 B. M. Trost and F. D. Toste, *J. Am. Chem. Soc.*, 1999, **121**, 3543–3544.
- 82 B. M. Trost, R. C. Bunt, R. C. Lemoine and T. L. Calkins, *J. Am. Chem. Soc.*, 2000, **122**, 5968–5976.
- 83 M. Fañanás-Mastral and B. L. Feringa, *J. Am. Chem. Soc.*, 2010, **132**, 13152–13153.
- 84 H. You, E. Rideau, M. Sidera and S. P. Fletcher, *Nature*, 2015, **517**, 351–355.
- 85 E. Rideau and S. P. Fletcher, *Beilstein J. Org. Chem.*, 2015, **11**, 2435–2443.
- 86 E. Rideau, H. You, M. Sidera, T. D. W. Claridge and S. P. Fletcher, *J. Am. Chem. Soc.*, 2017, **139**, 5614–5624.
- 87 A. Streitwieser, E. G. Jayasree, F. Hasanayn and S. S.-H. Leung, *J. Org. Chem.*, 2008, **73**, 9426–9434.
- 88 M. Sidera and S. P. Fletcher, *Chem. Commun.*, 2015, **51**, 5044–5047.
- 89 J.-B. Langlois and A. Alexakis, *Chem. Commun.*, 2009, 3868.
- 90 J.-B. Langlois and A. Alexakis, *Adv. Synth. Catal.*, 2010, **352**, 447–457.
- 91 J.-B. Langlois, D. Emery, J. Mareda and A. Alexakis, *Chem. Sci.*, 2012, **3**, 1062–1069.
- 92 L. B. Delvos and M. Oestreich, *Synthesis*, 2015, **47**, 924–933.
- 93 Y. Ge, X. Cui, S. M. Tan, H. Jiang, J. Ren, N. Lee, R. Lee and C. Tan, *Angew. Chem., Int. Ed.*, 2019, **58**, 2382–2386.
- 94 J. Li, X. Song, F. Wu, H. You and F.-E. Chen, *Eur. J. Org. Chem.*, 2022, **2022**, e202200860.
- 95 J. Liao, S. Zhang, Z. Wang, X. Song, D. Zhang, R. Kumar, J. Jin, P. Ren, H. You and F.-E. Chen, *Green Synth. Catal.*, 2020, **1**, 121–133.
- 96 J. Liao, X. Jia, F. Wu, J. Huang, G. Shen, H. You and F.-E. Chen, *Org. Chem. Front.*, 2022, **9**, 6640–6645.
- 97 J. Wang, J. Li, Y. Wang, S. He, H. You and F.-E. Chen, *ACS Catal.*, 2022, **12**, 9629–9637.
- 98 L. Wan, G. Kong, M. Liu, M. Jiang, D. Cheng and F. Chen, *Green Synth. Catal.*, 2022, **3**, 243–258.
- 99 L. Capaldo, Z. Wen and T. Noël, *Chem. Sci.*, 2023, **14**, 4230–4247.
- 100 X. Song, J. Qing, J. Li, X. Jia, F. Wu, J. Huang, J. Jin and H. You, *Chin. J. Org. Chem.*, 2023, **43**, 3174.
- 101 J. Li, X. Song, Y. Wang, J. Huang, H. You and F.-E. Chen, *Chem. Sci.*, 2023, **14**, 4351–4356.
- 102 J. T. Han, S.-T. Kim, M.-H. Baik and J. Yun, *Chem.–Eur. J.*, 2020, **26**, 2592–2596.
- 103 I. Sánchez-Sordo, A. Chaves-Pouso, J. Mateos-Gil, E. Rivera-Chao and M. Fañanás-Mastral, *Chem. Catal.*, 2023, **3**, 100730.
- 104 T. Suzuki, *Tetrahedron Lett.*, 2017, **58**, 4731–4739.
- 105 H. Weißbarth, F. Mühlhaus and A. Gansäuer, *Synthesis*, 2020, **52**, 2940–2947.
- 106 Y. Xu, T.-Y. Zhai, Z. Xu and L.-W. Ye, *Trends Chem.*, 2022, **4**, 191–205.
- 107 P.-J. Yang and Z. Chai, *Org. Biomol. Chem.*, 2023, **21**, 465–478.
- 108 C.-J. Yang, L. Liu, Q.-S. Gu and X.-Y. Liu, *CCS Chem.*, DOI: [10.31635/ccschem.024.202403839](https://doi.org/10.31635/ccschem.024.202403839).
- 109 U. Piarulli, P. Daubos, C. Claverie, M. Roux and C. Gennari, *Angew. Chem.*, 2003, **115**, 244–246.
- 110 U. Piarulli, C. Claverie, P. Daubos, C. Gennari, A. J. Minnaard and B. L. Feringa, *Org. Lett.*, 2003, **5**, 4493–4496.
- 111 H. Ito, T. Okura, K. Matsuura and M. Sawamura, *Angew. Chem., Int. Ed.*, 2010, **3**, 560–563.
- 112 A. Vázquez-Romero, J. Rodríguez, A. Lledó, X. Verdager and A. Riera, *Org. Lett.*, 2008, **10**, 4509–4512.
- 113 Y. Yasuda, H. Ohmiya and M. Sawamura, *Angew. Chem., Int. Ed.*, 2016, **55**, 10816–10820.
- 114 S. S. Goh, S. Guduguntla, T. Kikuchi, M. Lutz, E. Otten, M. Fujita and B. L. Feringa, *J. Am. Chem. Soc.*, 2018, **140**, 7052–7055.
- 115 S. S. Goh, P. A. Champagne, S. Guduguntla, T. Kikuchi, M. Fujita, K. N. Houk and B. L. Feringa, *J. Am. Chem. Soc.*, 2018, **140**, 4986–4990.
- 116 R. Jacques, R. D. C. Pullin and S. P. Fletcher, *Nat. Commun.*, 2019, **10**, 21.
- 117 N. A. Butt and W. Zhang, *Chem. Soc. Rev.*, 2015, **44**, 7929–7967.
- 118 J. Mateos, N. Fuentes-Vara, L. Fra, E. Rivera-Chao, N. Vázquez-Galiñanes, A. Chaves-Pouso and M. Fañanás-Mastral, *Organometallics*, 2020, **39**, 740–745.
- 119 R. He, X. Huo, L. Zhao, F. Wang, L. Jiang, J. Liao and W. Zhang, *J. Am. Chem. Soc.*, 2020, **142**, 8097–8103.
- 120 W.-Y. Huang, C.-H. Lu, S. Ghorai, B. Li and C. Li, *J. Am. Chem. Soc.*, 2020, **142**, 15276–15281.
- 121 L. Zhao, G. Li, R. He, P. Liu, F. Wang, X. Huo, M. Zhao and W. Zhang, *Org. Biomol. Chem.*, 2021, **19**, 1955–1959.
- 122 L. Xiao, X. Chang, H. Xu, Q. Xiong, Y. Dang and C.-J. Wang, *Angew. Chem., Int. Ed.*, 2022, **61**, e202212948.
- 123 B.-K. Zhu, H. Xu, L. Xiao, X. Chang, L. Wei, H. Teng, Y. Dang, X.-Q. Dong and C.-J. Wang, *Chem. Sci.*, 2023, **14**, 4134–4142.

